Proceedings of the
Annual Stability Conference
Structural Stability Research Council
Toronto, Canada, March 25-28, 2014

Stability and Service Consideration for Steel Bridge Orthotropic Deck Panels

M.W. Jen[1], B.T. Yen[2]

Abstract
Due to the relatively lighter weight, steel orthotropic panels with the main plate reinforced with longitudinal stiffening ribs have been used as compressive components in structures such as ships and bridges. The goal of lighter weight led to the tradition of selecting thin steel plate components including the main plate and the webs of the reinforcing ribs. Resent increase in application of such panels as bridge decks reveals the conditions of possible damage in fatigue cracking due to service condition under truck loads. The wheels of trucks on the deck generate relatively high magnitude of local stresses in the main plate of the steel deck and in the webs of the stiffening ribs due to out-of-plane displacement of the plates. A recently designed orthotropic deck suggests that component plates slightly thicker than the currently prevalent ones can satisfy the requirement of lighter weight and simultaneously reduces the plate-bending stresses due to the out-of-plane displacement of these plates. This paper examines the local buckling of the rib walls and the strength of the ribs, presents a procedure for estimating the compressive strength of steel orthotropic deck panels under truck loads, examines the stability of the stiffened deck against overall buckling and compares relatively the stresses due to plate-bending.

1. Introduction

Longitudinal stiffening ribs of steel orthotropic decks are continuous components of the deck system. Trapezoidal-shaped ribs are most common in this country. These ribs are primarily subjected to compressive forces from the global action of the bridge deck and to bending moments from the local loads of the trucks on the deck.

Current provisions in the AASHTO LRFD Bridge Design Specifications permit that trapezoidal-shaped longitudinal stiffening ribs are designed as individual columns with a simply supported condition at transverse diaphragms (AASHTO). The cross sectional dimensions of a rib column and the thickness of its component plates must conform to a dimensional condition specified by an equation (Eq. *9.8.3.7.2-1* of AASHTO) for controlling the out of plane flexural stresses of the rib walls and the associated possible development of fatigue cracks. Practically, buckling stress of the rib walls is the controlling factor for design.

[1] Principal Engineer, Parsons Transportation Group, New York, NY, USA. <mark.jen@parsons.com>
[2] Professor Emeritus, Civil Engineering, Lehigh University, Bethlehem, PA, USA. <bty0@lehigh.edu>

The specifications also state that, for ribs with a span not more than *20 ft*, the effects of loads from trucks on the deck may be calculated from wheel loads placed over one rib only. The combination of local and global effects should be considered at the strength limit state. At the ends of a rib over the diaphragms of the deck, there is negative longitudinal bending moments in the rib which increase the compressive stresses in its walls. This condition may compromise the compressive strength of the ribs.

Results from an experimental examination of trapezoidal-shaped ribs confirmed the importance of considering the continuity of ribs in evaluating the flexural behavior of the ribs and the deck (Jen and Yen 2006). The more important finding from this study is that the column behavior of stiffening ribs under compressive forces and the beam-column behavior of these ribs subjected to compression and wheel load-induced bending moments, are practically identical. The failure mode consists of local bulging (buckling) of the rib walls and yielding of the rib cross section at the ends of the ribs. This finding has led to a practical procedure of "***sum of strength of parts*** (SSP)" for estimating the load carrying strength of the ribs.

The SSP procedure utilizes the condition that the yield stress (yield point) for thinner steel plates is usually higher than that for thicker plates of the same grade. For example, the yield stress of a *5/8 in*. thick deck plate of Grade *50* steel is nominally *50 ksi* while that of a *5/16 in*. thick rib wall of the same grade of material usually approaches *70 ksi*. The effects of the negative bending moment at the ends of rib columns due to the wheel loads of trucks are not significant and can be considered as being compensated by the higher yield point when the specified yield stress of *50 ksi* in the design process is used (Jen and Yen 2008).

The most widely used longitudinal stiffening ribs are trapezoidal shaped, closed ribs. The longitudinal stiffening ribs' load carrying capacity is controlled by the rib buckling strength. The relatively simple procedure of estimating the compressive strength of a rib by the sum of its component strength has been proposed. Based on these, and with consideration of the interaction of axial compression, shear and flexure, the orthotropic deck panel strength can be evaluated. This suggested procedure for computing the global strength of orthotropic deck panels considers the shear lag, local buckling and global buckling of steel component plates. The procedure can help design engineers to estimate the deck panel strength and optimum the design for orthotropic deck panels (Jen and Yen 2013).

2. Results from Experimental Program Study

To determine the strength of decks a serial of tests and finite element analyses were carried out. First are the influence surface tests, which were to obtain the baseline measurements on the response of deck system to static loads. These are the response and behavior of a deck system and its components under local wheel loads. The bending tests were to explore the failure modes of the deck system and its components due to the vertical traffic loading. The column test and beam-column tests were to define the load carrying capacity of the deck system and its components due to global compression force.

A. Influence Line and Surface

The establishment of influence lines for the design of bridge deck subjected to live loads (wheel loads) allow the determination of the maximum moment, shear and axial forces, etc. for a given cross section in a bridge member under live loads, as shown in Figure 1.

In the experimental phase, there were 4 actuators in a line at position 1 to 4 in the longitudinal direction. The actuators could be moved to 5 different locations transversely. The strain distributions on the bottom of deck plate along Diaphragm A1 when the simulated where load was at different position on Line 6 are plotted in Figure 1. Line 6 was along the mid width of Rib 8. With *80 kips* (*489.3 kN*) applied at Position 1 directly over Diaphragm A1, the maximum stress on the bottom of the deck at Rib 8 was not the highest. The highest stress of about 7 ksi (*48 MPa* at *230 μin./in.* strain) occurred when the load was at Position 2 between Diaphragm A1 and B. When the *80 kips* (*489.3 kN*) load was at Position 3 over Diaphragm B, the stresses at the strain gages were practically zero. When the load was at Position 4 between two Diaphragms, the bottom of the deck plate was in low tension at the junction with the rib wall at Ribs 8, 9 and 10. It was possible to applied loads simultaneously to simulate multiple axles. This was done with actuators at Positions 3 and 4, and 2, 3, and 4. The strain distribution under these load combinations are also given in Figure 1. The elastic behavior of the deck and the capability of strain (stress) superposition were confirmed.

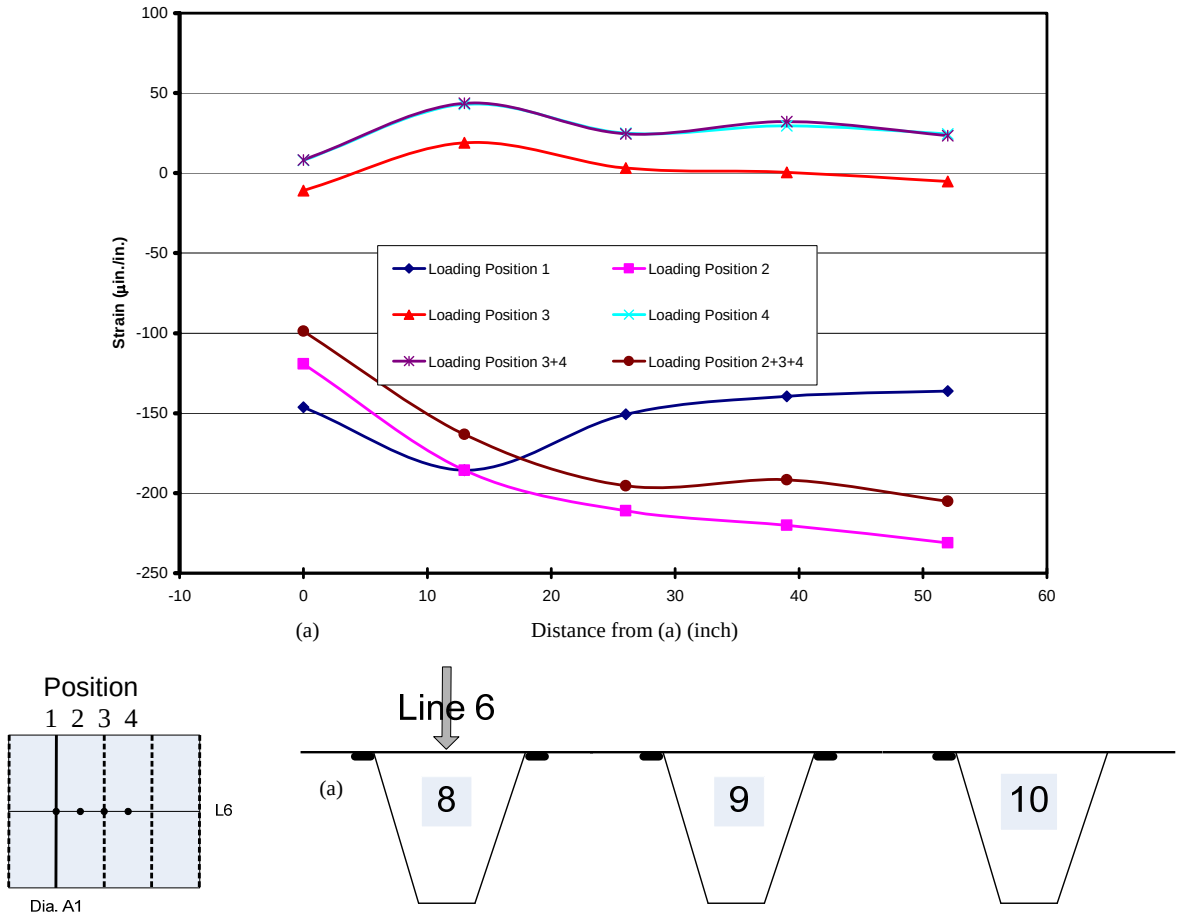

Figure 1: Strains on the bottom of deck plate along Diaphragm A1 (loads on Line 6)

Figure 2 shows the strain readings on a floorbeam web at the top of the cutouts when loads were applied at various loading lines. Presented are the variations of stresses on Diaphragm B at the cutouts of Ribs 6 to 9 for loading Position 2 of Loading Line 1 to 5.

Compose multiple influence lines, the influence surface scan be corresponding multiple influence lines. The influence surfaces for strains on the wall of Rib 6 inside the cutout at Diaphragm B are presented in Figures 3 and 4. The influence surfaces do not have an identical shape because the stresses on the surfaces of the rib wall are the combination of membrane (in plane) and plate (out of plane) bending stresses. The important phenomenon is that the wheel load affects primarily only the rib directly under the wheel, and only slightly the adjacent rib.

The measured and computed stresses in the model orthotropic deck indicate that in the transverse direction of the deck, primarily only one rib carries the simulated wheel load of a truck. By considering that the transverse distance between wheels of the same axle of a AASHTO truck (*72 in., 1829 mm*) or parallel trucks is more than the width of two ribs of the deck panel (*2 × 26 = 52 in., 1321 mm*), it can be concluded that only wheel loads need to be considered in the evaluation of stresses and strength of ribs.

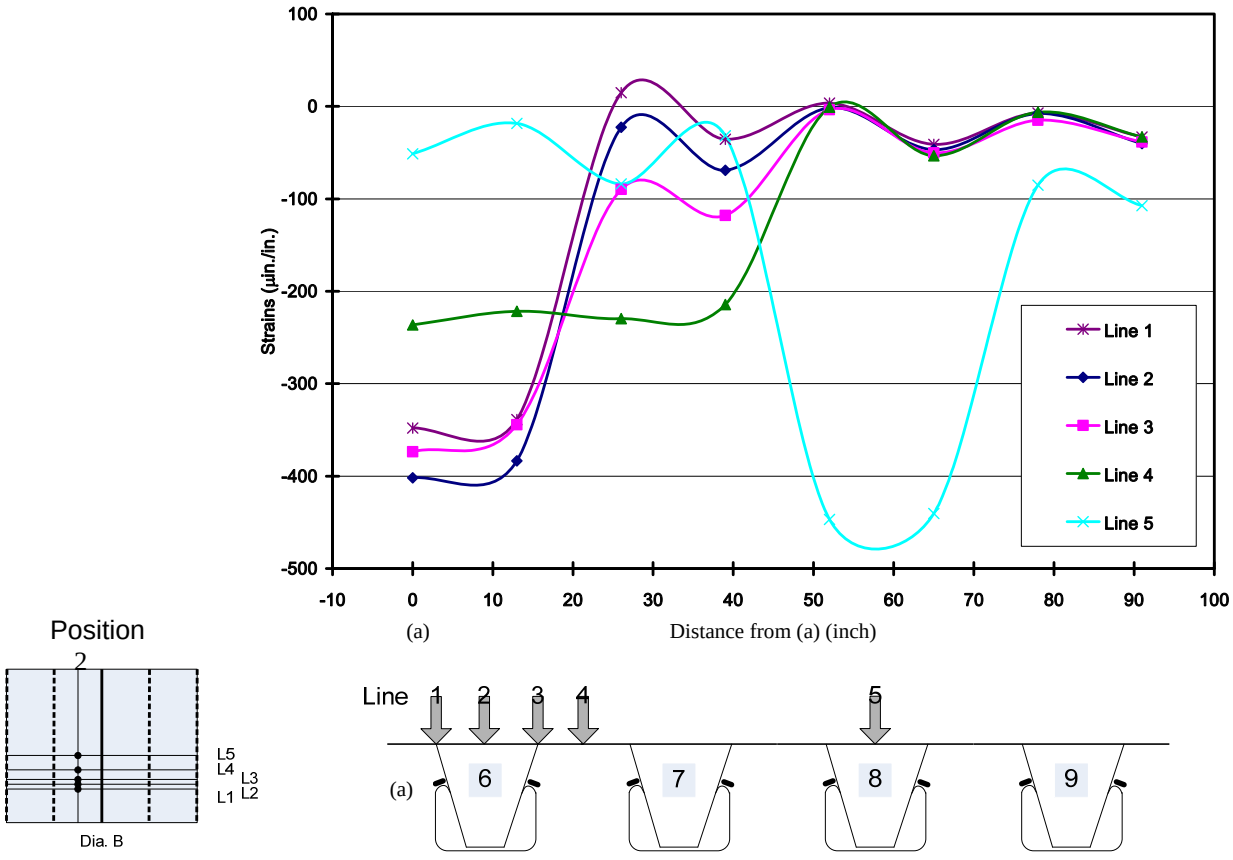

Figure 2: Strains at cutout on the South face of Diaphragm B (Loading Position 2)

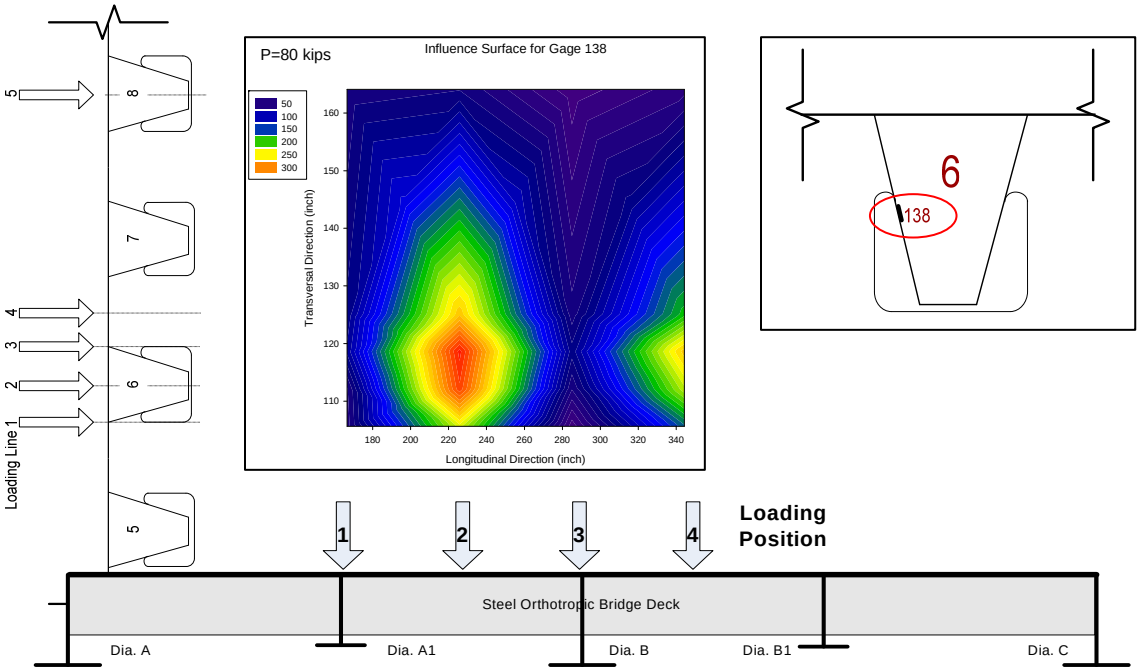

Figure 3: Influence Surface of Strain on Rib Wall Interior Face at Diaphragm B

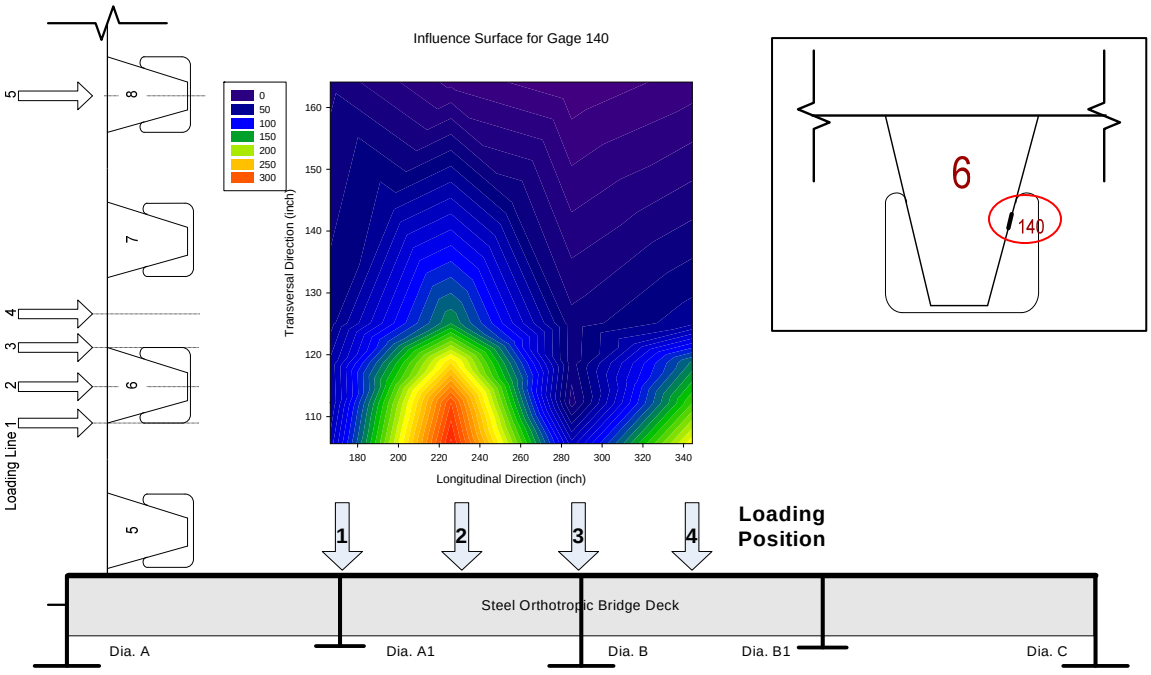

Figure 4: Influence Surface of Strain on Rib Wall Interior Face at Diaphragm B

From the experimental results with an applied load of *80 kips* (*356 kN*) which is four times the HS 25 wheel load, all response of stresses are in the linear elastic range. This indicates the adequacy of superposition of multiple wheel loads in the longitudinal direction and the utilization of influence line for beams. In the subsequent evaluation on the strength of ribs, it is

conservative to assume (as it does in design specifications) that wheel loads are supported transversely by only one rib. In the longitudinal direction, multiple simulated wheel loads were applied during testing. Because of the difference in stiffness of the diaphragms with or without floorbeams, the effect of longitudinal load position was strong on the local stresses of the diaphragms and adjacent rib walls.

B. Bending test

Three-support single loading point static bending tests were made to determine the bending strength and failure mechanism of single- and triple-rib beam members. The setup is shown in Figure 5. The results of the experiment showed that the rib beams failed with the rib wall plate buckled locally near the floorbeams. The deflection shaped after the test is shown in Figure 6.

The partial deck panels which were supported on three sides and free on the fourth, behaved linearly under a simulated wheel load up to *300 kips* (*1335 kN*) in the panel. The behavior was slightly nonlinear when the load was in the partial panel with the rib connections, and when two simultaneous loads were in the two adjacent panels. One or two *300 kips* (*1335 kN*) loads applied on a triple-rib continuous beam, which was isolated from the partial deck, induced similar behavior as that of the partial deck panel.

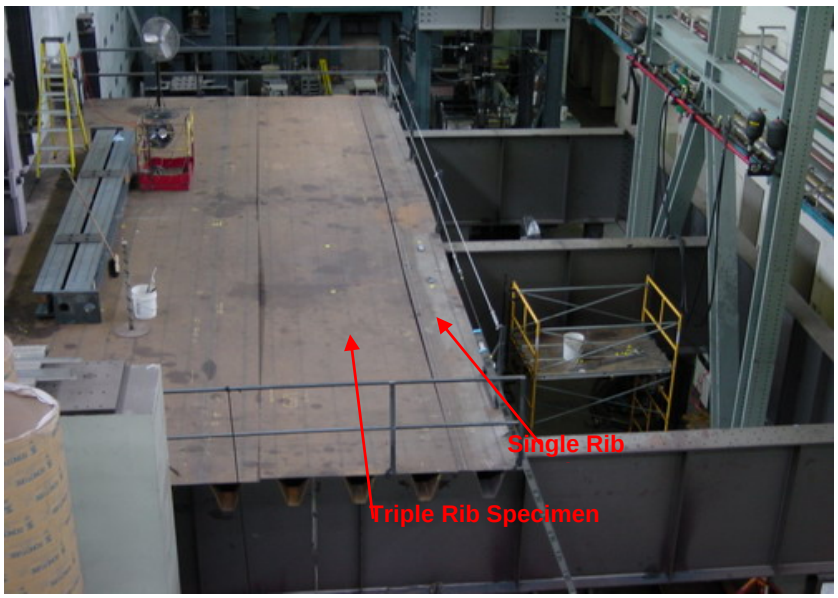

Figure 5: Bending tests specimens on partial deck

The isolated single-rib continuous beam sustained a maximum vehicular wheel load of *162 kips* (*720 kN*) in one span with failure located at the rib connection in the other span. A similar triple-rib beam sustained *591 kips* (*2631 kN*), being slightly higher than three times the single-rib beam strength. This condition indicates the participation of all ribs of the triple-rib beam in carrying loads placed on one rib. Analysis by finite element models indicates that the strength of each rib without a connection would be *300 kips* (*1335 kN*) or higher.

The magnitude of *300 kips* (*1335 kN*), being the maximum applied load on the partial deck panels as well as the flexural load strength of each rib, is 15 times the HS 25 wheel load of *20*

kips (*89 kN*). With the conclusion from the influence surface tests that wheel loads affect primarily only one rib, and that wheel loads of the same axle are two or more ribs apart, it can be concluded that axle loads of HS 25 trucks do not cause problem with respect to static flexural strength of the ribs of the model deck.

Figure 6: Closed up view of buckled rib wall of triple-rib Beam

C. Column and Beam-column tests

Although the instability problem of the orthotropic steel deck system due to flexural compressive stress has been recognized for years, current bridge design specifications do not clearly specify the criteria to prevent local buckling of the orthotropic deck system. Most previous studies on orthotropic steel deck systems were focused on the out-of-plane behavior of the steel deck, only limited study has been carried out on the in-plane compressive behavior of the orthotropic steel deck system. There is a lack of knowledge on the inelastic behavior of the orthotropic steel deck system under flexural compressive stress.

Four compressive specimens were tested in this study. All four were *18 ft.* long, with two cut-off diaphragms *5 ft.* from the mid-length, or *4 ft.* form the ends. The width of the deck plate of a single-rib was *26 in.* The width of the top of a trapezoidal rib is *13 in.*; the bottom is *5 in.* including the curved transition of the wall. It is *4.67 in.* without. The thickness of the deck plate was *5/8 in.*; the rib, *5/16 in.* one single-rib specimen was tested in compression (column) and two in compression with a transverse load simulating a wheel of a truck on the deck (beam-column). The effect of bending induced by the wheel on the behavior of the beam-column was not significant. Failure of all four specimens was due to inelastic local buckling of the rib walls. The triple-rib beam-column was practically equivalent to the sum of three single-rib beam-columns.

Figure 7: Column and beam-column tests setup (Left: single-rib column test, Middle: single-rib beam-column test, Right: triple-rib beam-column test)


Figure 8: Column and beam-column test failure modes, local buckling at deck plate, rib and yield lines on the deck plate

A single-rib and triple rib beam-column specimens in the test machine is shown in Figure 7. Axial compressive forces were applied monotonically to failure of the specimens. For the beam-column specimens, a transverse force of *40 kip*s, representing twice the wheel load of a HS25 truck was applied at the axial force of *300 kips*. The *40 kips* force was induced by a hydraulic jack through a pad simulating the foot print of the truck wheel.

With the given dimensions and the mechanical properties, the nominal axial force corresponding to first yield at the deck plate (P_y) of the single-rib column, SC, was *1367 kips*. For the single-rib beam columns SBC1 and SBC2 it was *1134 kips*, and for the triple-rib beam column TBC it was three time that, being *3402 kips*. Without consideration of local buckling of the rib, the axial force for yielding of the complete cross section (P_p, the "plastic' compressive strength) of a single column was *1576 kips*. Without the *40 kips* transverse load the corresponding required axial force for full yielding of a triple-rib column would be *4729 kips*. The failure modes are shown in Figure 8.

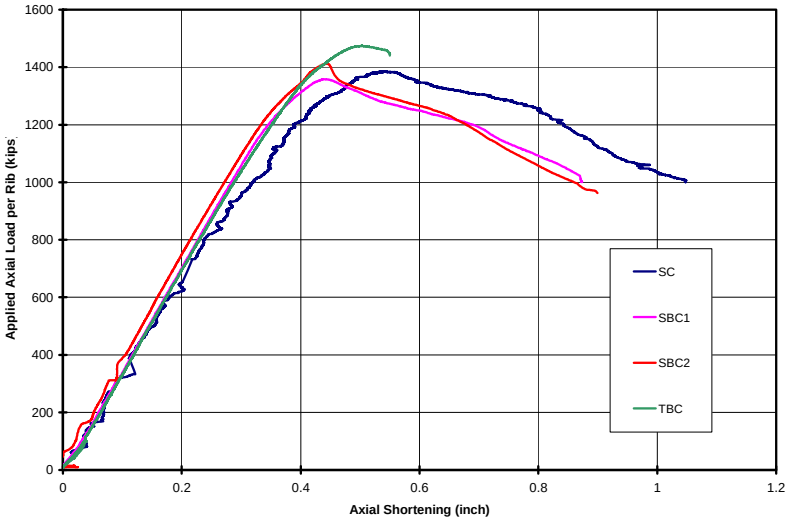

Figure 9: Axial shortening of column and beam-column tests

Strain gages were placed on the deck plate and rib wall of the specimens, primarily at the middle half of the column length. The overall shortening of the test members was measured by LVDTs placed between the column end plates. Most of the LVDTs for measuring lateral displacement were located against the rib bottom opposite the simulated wheel load. Figure 9 shows the load-displacement of the specimens.

The primary reason that the beam-column and column specimens of the rib behaved very similar is the insignificant magnitude of the lateral load. The applied lateral load of *40 kips* (*178 kN*), even though it is twice that of the wheel load of a HS 25 truck, is very low in comparison to the maximum applied axial load of around *1400 kips* (*6230 kN*) to each of the ribs of the specimens. The *40 kips* load generated bending moments in the beam-columns, but the magnitudes of the moment were not high enough to induce overall beam-column action. Rather, failures were due to local buckling of the rib walls.

3. Finite Element Analysis

Nonlinear finite element program ABAQUS was used to analysis the specimens. The finite element models are shown in Figure 10. Test results compared well with those by the finite element analysis. Figure 11 shows the results of the triple rib specimen.

The computed load carrying capacity or maximum loads of the test specimens by the finite element analysis are listed in Table1. The computed maximum load for the single-rib beam-columns is very close to the average of the two test specimen, being *1381 kips* versus *1385 kips*. For the triple-rib specimen TBC the computed value of *4041 kips* is lower than the test result of *4422 kips*, being on the conservative side. The experimental maximum load for the single-rib column is lower than the computed value. This is attributed to the condition that the specimen was cut out from the prototype deck along a longitudinal welded joint which would have introduced residual stresses in this specimen. The distribution and magnitudes of these residual stresses were assumed, shown in Figure 12 and included in the analyses.

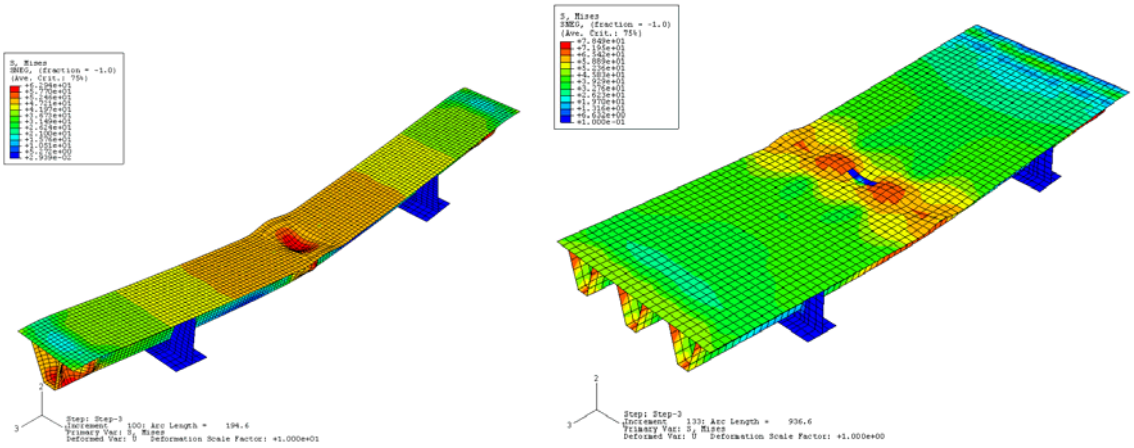

Figure 10: Finite element analysis models for single and triple rib beam-column tests

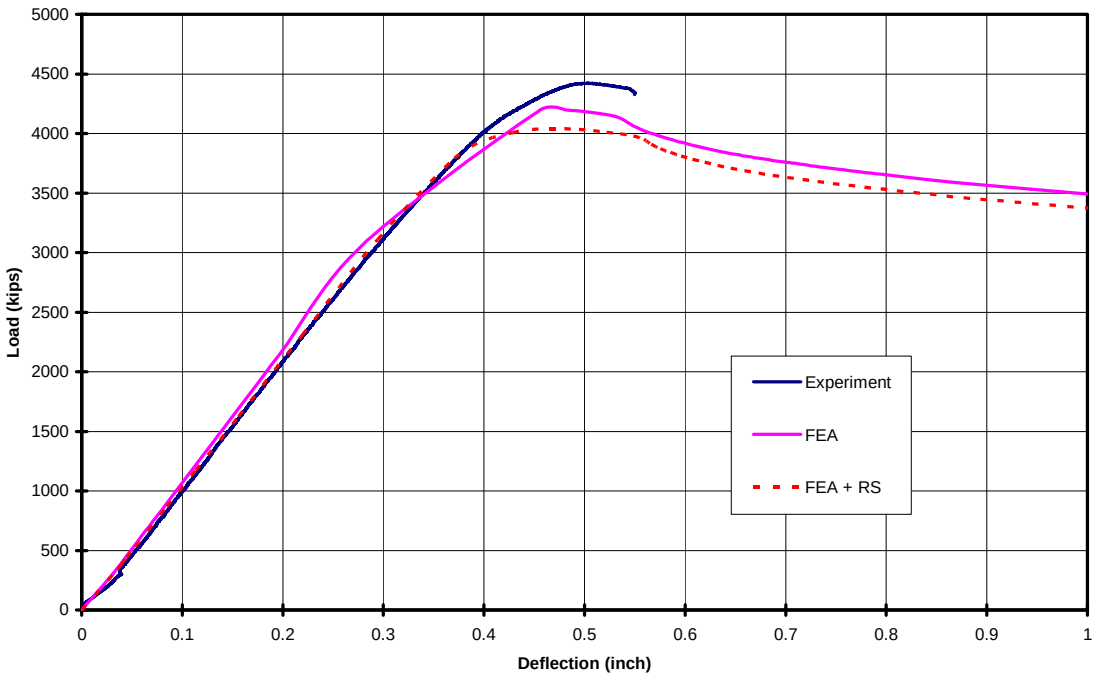

Figure 11: The triple beam-column FEA and experimental results

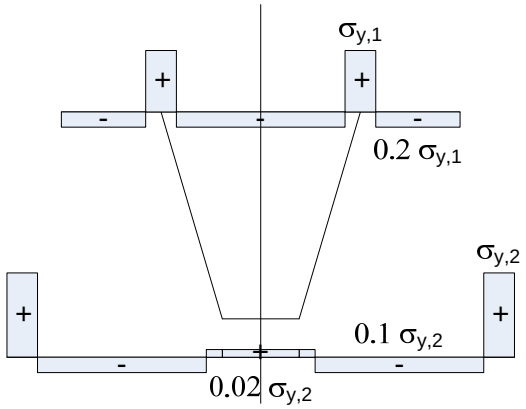

Figure 12: Residual stress pattern for finite element analysis

The results of computed ultimate loads by the finite element analysis are listed with the experimental results in Table 1. The finite element analysis (FEA) included two cases: a) incorporated only the overall initial out of straightness of the specimens with no consideration of residual stresses and b) included both. For all four specimens the inclusion of residual stresses resulted in only a slightly lower computed strength. The highest deviation is about 4%. This indicates that the presence of residual stress has only minor effect on the load carrying capacity of the column and beam-columns. In comparison with the experimental results, the computed strength with consideration of residual stresses are generally closer to the recorded ultimate loads of testing, with an overestimate of the column strength and slight underestimate of the beam-column strength.

Table 1: Experimental and FEA Results

Specimen	Ultimate Load (kips)				Max. Axial Deflection (inch)		
	Exp.	FEA		Difference (b) (%)	Exp.	FEA	
		(a)	(b)			(a)	(b)
SC	1385	1578	1546	11.6	0.542	0.512	0.519
SBC 1	1358	1441	1381	1.6	0.440	0.448	0.453
SBC 2	1412	1441	1381	-2.2	0.463	0.448	0.453
TBC	4422 (1474)	4198 (1399)	4041 (1374)	-8.6	0.503	0.481	0.464

(a) without consideration of residual stresses.
(b) with consideration of residual stresses.

The maximum wheel loading did not affect the results of single-rib beam-column. For the evaluation of load carrying capacity of single rib and deck panel, the truck wheel loading can be ignored.

The experimental and analytical results of the single-rib column and beam-columns were very similar. So were the results from single-rib and triple-rib beam-columns. Failure of the specimens at ultimate load was by local buckling of the rib walls and yielding of the deck plate. There was no overall buckling of the ribs.

An analytical procedure of estimating the compressive strength of a rib column by the sum of its component strength has been formulated as shown below.

4. *Sum of Strength of Parts* (*SSP*) Method for Deck Strength Evaluation

The load-carrying compressive strength of a single trapezoidal-shaped stiffening rib in an orthotropic deck is to be computed as the sum of the compressive strength of its component parts. These parts are the portions of the deck plate attributed to the rib, the two inclined webs of the rib and the bottom flange of the trapezoidal shape, as shown in Figure 13.

Because the deck plate is always thicker than the rib wall and the distance between the webs is usually less than the depth of the inclined webs, buckling of the webs would occur before the buckling of the deck plate. Consequently, inelastic buckling of the webs and yielding of the deck plate are the references for design strength. The bottom flange of the rib would reach yielding at the same time as does the deck plate.

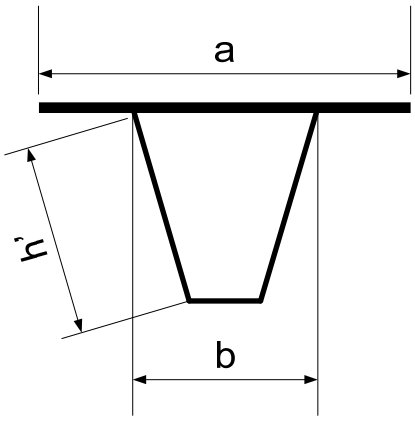

Figure 13: Show dimensions of components, a , b , h'

Following the guidelines of the Design Manual for Orthotropic Steel Plate Deck Bridges (Wolchuk, AISC 1963) the elastic buckling stress (f_{cre}) of a simply supported web plate under uniform compression is given by Eq. 1. With consideration of residual stresses in the ribs and with adoption of the relationship between elastic and inelastic modulus of the material by Bleich (1952), the inelastic buckling stress (f_{cri}) can be approximated by Eq. 2 as a function of f_{cre} and the yield stress, f_y (AASHTO).

$$f_{cre} = k\frac{\pi^2 E}{12(1-\nu^2)}\left(\frac{t}{h}\right)^2 \quad \text{for } k = 4 \tag{1}$$

$$\frac{f_{cri}}{f_y} = \frac{1}{1+0.1875(\frac{f_y}{f_{cre}})^2} \tag{2}$$

The compressive strength of the rib (P_u) can then be estimated by the following equation.

$$P_u = 2\cdot f_{cri}\cdot h'\cdot t_r + 2\cdot f_y\cdot a\cdot t_d + f_y\cdot b\cdot t_r \tag{3}$$

An analytical procedure of estimating the compressive strength of rib columns developed to check the application of *SSP*. The rib models were developed and analyzed using the software ABAQUS (2005). Models of single, triple, five, seven and sixteen ribs were studies.

The results are listed in Table 2. As the number of ribs increase, the computed strength per rib increase slightly as the effect of free edges diminishes. With the increases of number of ribs, the ductility increases tremendously. The computed single rib compressive strength (P_u) by Eq. 3 is *1602 kips*. This is almost exactly the average strength per rib by the finite element model which incorporates residual stresses.

The results of stress distribution of 16-ribs are shown in Figure 14, at an axial deflection of about *1 in.* (*25 mm*). From the 16-rib model it is seen that there were slight variation of stresses among the ribs although the model was loaded uniformly at one end.

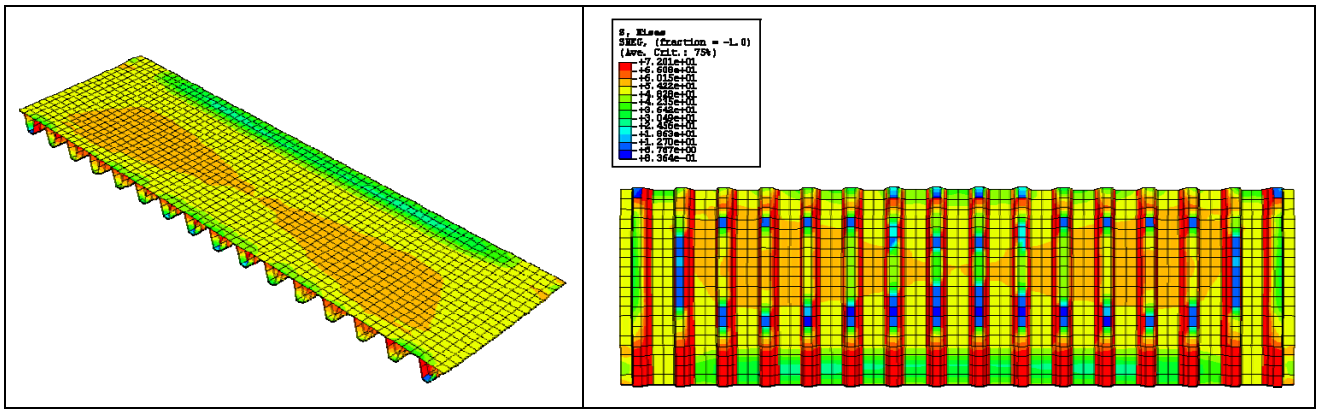

Figure 14: Sixteen-Rib Finite Element Model

Table 2: Summary of Rib Strength by Model

Number of Ribs N	P_u / N (kips)	$(P_u / N) / P_{u1}$ (%)	Axial Deflection at P_u (inch)
1	1357	100.00	0.338
3	1357	100.00	0.338
5	1545	113.90	0.397
7	1564	115.31	0.394
16	1603	118.18	0.274

(P_u for single rib by *SSP* Method = *1602 kips*)

Considering that deck panels are not subjected to uniform end forces, rather there are the effects of shear lag, of variations of boundary conditions, and of initial imperfection of plate components and rib stiffeners, it is definite that the procedure of summation of parts can be applied for estimating the strength of deck panels. It is important to note that the elastic buckling strength of the 16-rib deck is very high, being beyond yielding of the deck.

5. Conclusions

The wheel loads of trucks are primarily carried by one trapezoidal-shaped stiffening rib. This is derived from the results of testing deck panels, ribs in bending and ribs under simultaneous compression and simulated wheel load, as well as from the results of finite element analysis.

In the experimental study, the behavior of single-rib and triple-rib specimens under the simulated wheel load and axial loads had similar behavior.

The experimental results were confirmed by using the finite element analysis with consideration of initial out-of-flatness of the rib wall and the overall out-of-straightness of columns. The analysis also permitted the evaluation of ultimate strength of rib columns.

The ultimate compression strength of ribs can be estimated by the procedure of sum of strength of parts (*SSP*). Finite element analysis results indicated that the buckling load of the deck panel was very high, being beyond the yielding of the deck. Overall buckling of the deck panel would not be a concern.

Acknowledgments

The authors acknowledge the assistance given by staff of Fritz Engineering Laboratory, and Center for Advanced Technology for Large Structural Systems (ATLSS) at Lehigh University. The research work was supported by Pennsylvania Infrastructure Technology Alliance (PITA) grants IART 043 and IART-056 projects.

References

AASHTO (2012), *AASHTO LRFD Bridge Design Specifications*, 6th Ed., American Association of State Highway and Transportation Officials, Washington D.C.

FHWA (2012). *Manual for Design, Construction, and Maintenance of Orthotropic Steel Deck Bridges*, Federal Highway Administration, Washington D.C.

AISC (1963). *Design Manual for Orthotropic Steel Plate Deck Bridges*, American Institute of Steel Construction. Chicago, IL.

SSRC (1998). Structural Stability Research Council, Guide to Stability Design Criteria for Metal Structures 5th Edition. Galambos, T. John Wiley and Sons Inc., New York, NY. ISBN 0-471-12742-6.

Jen, W.C., Yen, B.T. (2005), "Stress in Orthotropic Steel Deck Components Due to Vehicular Loads" *Proceedings of American Society of Civil Engineering Structures Congress*, New York City, USA, April 20-24.

Yarnold, M.T., Wilson, J.L, Jen, W.C., Yen, B.T. (2007). "Local Buckling Analysis of Trapezoidal Rib Orthotropic Bridge Deck Systems" *Bridge Structures: Assessment, Design, and Construction*, Volume 3, No. 2. Taylor and Francis.

Jen, W.C., Yen, B.T. (2008). Laboratory Study on Static Strength of Steel Orthotropic Deck Panel with Trapezoidal Stiffeners" *Proceedings of 2nd Orthotropic Bridge Conference* (2OBC), August 25-30.

Jen, W.C., Yen, B.T. (2013), "Compressive Strength of Orthotropic Deck Panels" *Proceedings of 3nd Orthotropic Bridge Conference* (3OBC), June 26-28.